Supporting Information for: Surface-particle interations control the escape time of a particle from a nanopore-gated nanocavity system: a coarse grained simulation.

Robert Zando[a], Mauro Chinappi[b], Cristiano Giordani[c], Fabio Cecconi[d], Zhen Zhang[a*]
[a] *Division of Solid State Electronics, Department of Electrical Engineering, Uppsala University, SE-751 03 Uppsala, Uppsala, Sweden.* [b] *Dipartimento di Ingegneria Industriale, Università di Roma Tor Vergata, Via del Politecnico 1, Roma, Italia.* [c] *Grupo Productos Naturales Marinos, Facultad de Ciencias Farmacéuticas y Alimentarias, Universidad de Antioquia, Calle 70 No. 52-21, Medellín 050010, Colombia.* [c] *Instituto de Física, Universidad de Antioquia, Calle 70 No. 52-21, Medellín 050010, Colombia.* [d] *Istituto Sistemi Complessi, CNR, Via dei Taurini, Roma, Italia.*

* mauro.chinappi@uniroma2.it, zhen.zhang@angstrom.uu.se

SUPPLEMENTARY NOTE S1: DERIVATION OF EQ. (4) OF THE MANUSCRIPT

Here we provide details on the derivation of the capture frequency k_c. The approach we used is often referred as Smoluchowski-like description and it was extensively used in estimating capture frequency in nanopores [S1–S3]. Other approaches were used in the literature to get similar results (see, among others [S4–S6]).

Let us consider a dilute solution of nanoparticles. The conservation equation for the solute concentration $C(\mathbf{r}, t)$ is

$$\frac{\partial C}{\partial t} = -\nabla \cdot \mathbf{J} \,. \tag{S1}$$

where $\mathbf{J}$ is the flux. In general, the flux has three components: i) the diffusive, ii) the phoretic, due to external forces acting on the solute particle and iii) the advection due to the solvent motion (that, it nanoconfined systems, can be induced by, for instance, electroosmosis [S7]). In this manuscript, we consider only the diffusion contribution that, for dilute solution, is

$$\mathbf{J} = -D\nabla C \tag{S2}$$

with D the diffusion coefficient. Eqs. (S1,S2) can be solved to get the time evolution of the concentration C and the flux $\mathbf{J}$ in the entire domain, once boundary and initial condition are defined.

2D case. The idealized system used to get an estimation for average dwell time τ for the surface diffusion (see Fig. 2b and Eq. (4), of the manuscript) is the 2D circular crown reported in Fig.S1. In the limit of large cavities and small aperture, we expect that this approach would provide a reasonable estimation of the capture rate independent of the actual shape of the cavity and of the apertures. We assume that the geometry has a radial symmetry with respect the origin of a Oxy plane. We indicated r as the distance from the origin and our domain is a circular crown bounded by an inner circle of diameter d_e, and an external circle of diameter d_{ext}. Our aim is to get an expression for the capture frequency in this simplified case. Thanks to the radial symmetry, all the quantities involved in Eqs. (S1,S2) depend only on r. Morevoer, we consider only cases where the diffusion coefficient D is homogeneous and constant. Consequently, Eqs. (S1,S2) reduce to

$$\frac{\partial C}{\partial t} = \frac{D}{r}\frac{\partial}{\partial r}\left(r\frac{\partial C}{\partial r}\right) \tag{S3}$$

that, in the stationary case and integrating over r becomes

$$D\frac{dC(r)}{dr} = \frac{A_{2D}}{r} \,, \tag{S4}$$

with A_{2D} a constant to be determined from the boundary conditions. It it worth noting that the Eq. (S4) is the radial component of the flux $\mathbf{J}$, so, integrating A/r on the surface of the inner boundary, we get the number of particles crossing the inner circle for unit of time, *i.e.* the capture frequency. In formula, this is expressed as

$$k_c = 2\pi A_{2D} \,. \tag{S5}$$

Here we use an adsorbing boundary at d_e while we assume that the concentration is fixed at the external boundary d_{ext}, *i.e.*

$$C(t, d_e) = 0 \quad , \quad C(t, d_{ext}) = C_0 \,, \tag{S6}$$

so, after simple manipulation, we get

$$A_{2D} = -C_0 D \ln \frac{d_{ext}}{d_e} \,. \tag{S7}$$

and, consequently

$$k_c = \frac{2\pi D C_0}{\ln \frac{d_{ext}}{d_e}} \tag{S8}$$

which is Eq.(4) of the manuscript.

3D case. Finally, we consider the 3D case. Now the idealized system is constituted by the domain between two concentric spheres: an adsorbing sphere of diameter d_e and external sphere of diameter d_{ext} where the concentration C_0 is fixed. Similarly, in 3D we assume that the system has radial symmetry. The equations (S3-S4) are now

$$\frac{\partial C}{\partial t} = \frac{D}{r^2}\frac{\partial}{\partial r}\left(r^2 \frac{\partial C}{\partial r}\right) \quad , \quad D\frac{dC(r)}{dr} = \frac{A_{3D}}{r^2} \,, \tag{S9}$$

and the capture rate, obtained integrating the radial flux on a hemisphere, is

$$k_{c,3D} = 2\pi A_{3D} \,. \tag{S10}$$

Unlike the 2D case, the A_{3D} now converges to a finite value for $d_{ext} \to \infty$ getting the standard Smoluchowski result

$$k_{c,3D} = \pi D C_0 d_e \,. \tag{S11}$$

This derivation is widely employed in capture and escape problems (for details and further applications, see, *e.g.* [S1–S3]). To obtain the formula proposed by Grigoriev [S8], the capture rate on a disk must be used. This amounts to a substitution of the prefactor π in Eq. (S11) with 2 [S9].

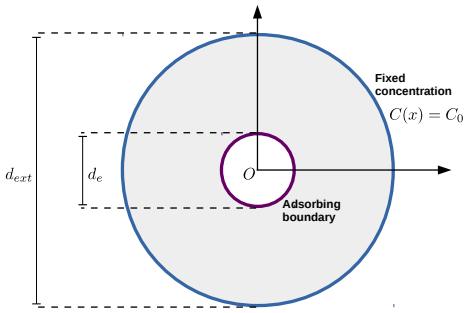

FIG. S1. Domain and boundary condition for diffusion equation in 2D. The domain, light gray, is a circular crown bounded by an inner circle of diameter d_e, where particles are adsorbed, and external circle of diameter d_{ext} where a fixed concentration C_0 is imposed.

SUPPLEMENTARY NOTE S2: DERIVATION OF EQ. (8) OF THE MANUSCRIPT

In this section, we provide a brief derivation of the average escape-time formula from an LJ well (Eq.(8) of the main text). With reference to Fig.S2, the escape process from a one dimensional LJ-well can be defined in the following setup: a particle is released at the minimum of LJ-well ($x_0 = 2^{1/6}\sigma$), and it performs a diffusion on the interval $[0, b]$. The boundary conditions require: 1) absorption at $x = b$ (removal of the particle as soon as it reached $x = b$), and 2) reflection at $x = 0$.

In the general formulation [S10, S11], the average first-arrival time at the boundary b for a particle released in x_0, is related to the survival probability,

$$S(x_0, t) = \int_0^b dx\; p(x, t|x_0)\,, \tag{S12}$$

where $p(x, t|x_0)$ denotes the probability density that a particle emitted in x_0 at time $t = 0$ is detected in x at time t. By definition, $S(x_0, t)$ is the probability that, at the time t, the particle has not yet left the interval $[0, b]$. Indeed, the integral

$$\tau(x_0) = \int_0^\infty dt\; S(x_0, t) \tag{S13}$$

is exactly the average escape-time from the interval $[0, b]$, if the particle starts from x_0. Without loss of generality we can safely drop the "0" index in the following.

$S(x, t)$ is known to satisfy the backward Kolmogorov equation [S10]

$$\frac{\partial S}{\partial t} = e^{\beta U(x)} D \frac{\partial}{\partial x}\left[e^{-\beta U(x)} \frac{\partial S}{\partial x}\right] \tag{S14}$$

with the boundary conditions $S'(0, t) = 0$ (reflecting) and $S(b, t) = 0$ (absorbing). A differential equation for $\tau(x)$ is obtained by integrating Eq.(S14) in the interval $0 \le t < \infty$, and taking into account that $S(x, \infty) = 0$ and $S(x, 0) = 1$, thus

$$\frac{d}{dx}\left[e^{\beta U(x)} \frac{d\tau}{dx}\right] = -\frac{e^{-\beta U(x)}}{D}. \tag{S15}$$

To find a unique solution, the above equation has to be completed with the obvious boundary values $\tau'(0) = 0$ and $\tau(b) = 0$, stating that the particle is reflected by the boundary $x = 0$ and that it is instantaneously absorbed at $x = b$. We are interested in the average first-exit time at $x = b$, from $x = x_0$. A first integration in the interval $[0, x]$ provides,

$$e^{\beta U(x)} \frac{d\tau}{dx} - e^{\beta U(x)} \frac{d\tau}{dx}\bigg|_0 = -\int_0^x dy \frac{e^{-\beta U(y)}}{D} \tag{S16}$$

where the second term of the l.h.s. vanishes because of the boundary condition, $\tau'(0) = 0$. A further integration, from x_0 to b, yields

$$\tau(x_0) = \frac{1}{D}\int_{x_0}^b dx e^{\beta U(x)} \int_0^x dy e^{-\beta U(y)} \tag{S17}$$

which is exactly Eq.(8) of the main text for $b = 4\sigma$ and $x_0 = 2^{1/6}\sigma$. As a final note, we remind the reader that here we used the generic symbol τ while in the main text τ is used for the dwell time in the cavity and τ_s is used for the typical time that a particle is trapped at the solid wall by the LJ-well.

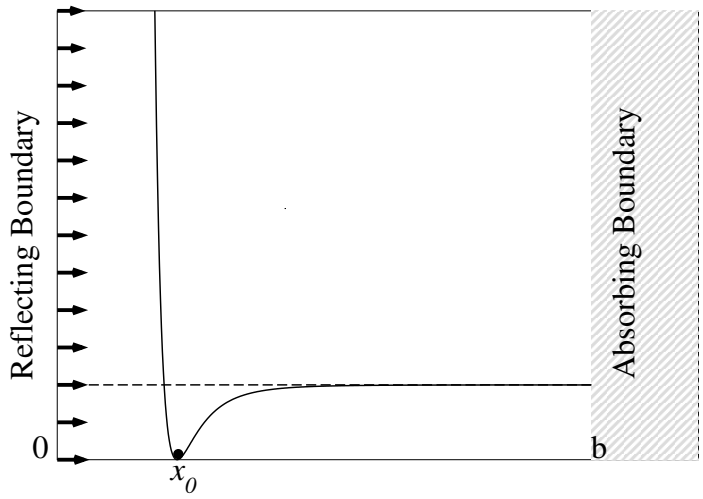

FIG. S2. Sketch of the physical setup used to compute the mean first exit-time from a LJ-well. A particle performing thermal diffusion is initially placed in the minimum of the LJ-potential, it is absorbed (removed) as soon as it crosses the boundary $x = b$. The other boundary, $x = 0$, has to be considered reflecting due to the high repulsion exerted by the steep tail of the LJ-potential.

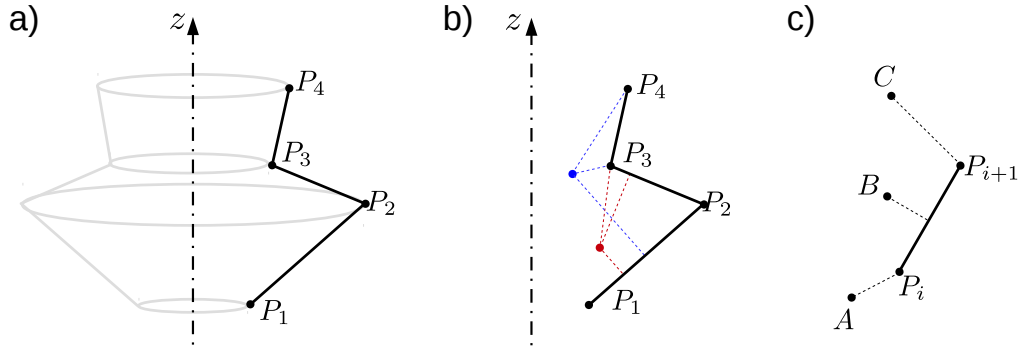

FIG. S3. Generation of confining potential for the Brownian model. a) The cavity profile is modelled as a sequence of connected segments in the plane $\rho - z$. The two extreme points of the i-th segment are indicated as P_i and P_{i+1}. These coordinates define the edges of the geometry cross-section. The confining geometry is obtained by the rotation of this line around the z axis. For the cavity geometry used in this study, four points must be specified. For instance, in the case of the cavity of Fig.1 of the manuscript ($d_c = 400$ nm, $d_e = 50$ nm), the points were $P_1 = (25, 200)$, $P_2 = (200, 200)$, $P_3 = (200, -200)$, $P_4 = (25, -200)$. b) The wall-particle interaction potential depends on the distance between the particle and the wall. To calculate the minimum distance of a point from the wall, we first calculate the distance between the point and each segments and, then, we select the minimum one, see red and blue points. c) Three examples of distance between a point and a segment. It is worth noting that the minimum distance is not always the length of the segment starting from the point and normal to the segment (as for point B) but it can also be the distance between the point and one of the two segment extremes as for points A and C.

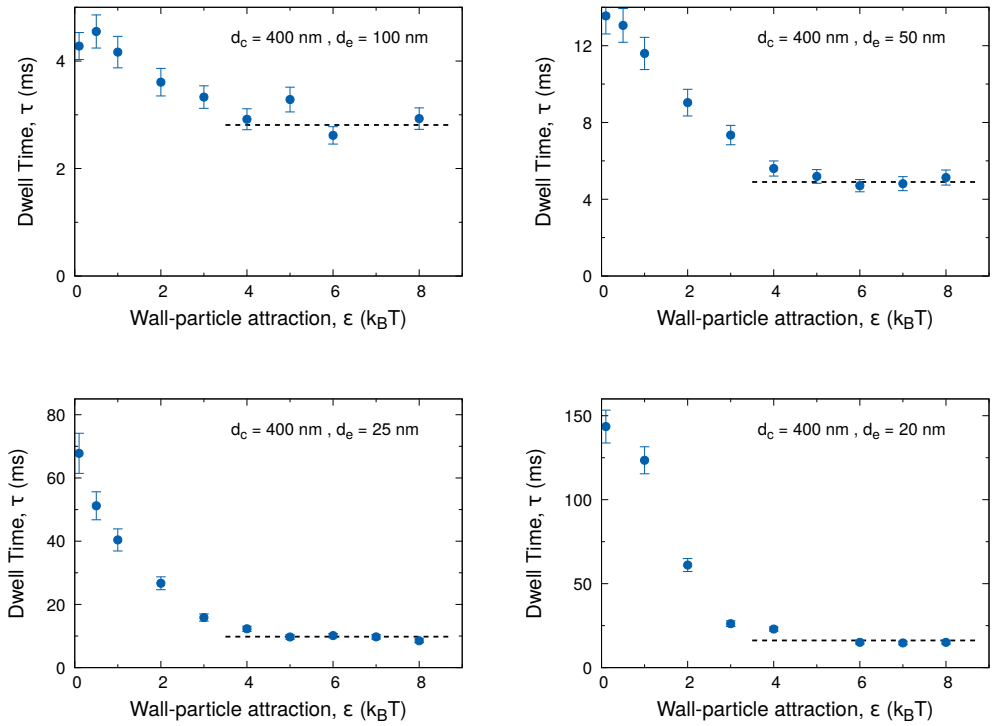

FIG. S4. Additional data on dwell time dependence with respect to particle-wall interaction. The simulations were run for a constant cavity volume with a varying aperture diameter d_e. In all cases, the trend is the same: the dwell time τ reaches a plateau for attractive wall, $\epsilon/k_BT > 4$. This plateau corresponds to a 2D surface diffusion process (see Fig.1 of the main text). Moreover, it is apparent that, as expected, the dwell time τ increases when the exit diameter d_e decreases.

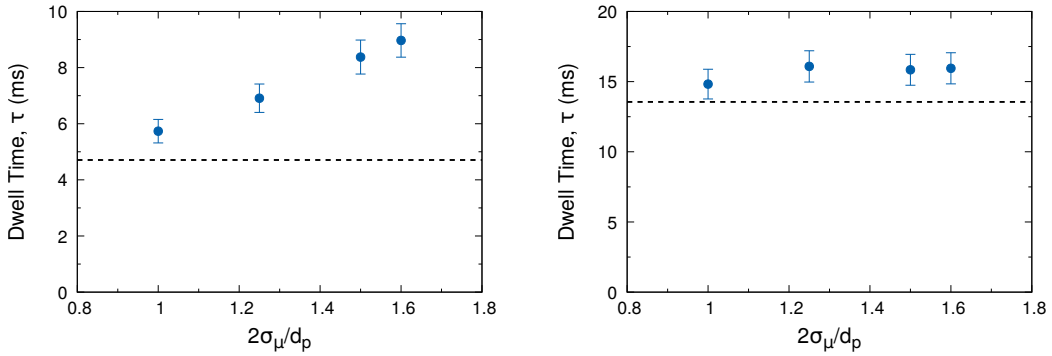

FIG. S5. Effect of the size σ_{mu} of the mobility reduction region. In order to determine the ways in which the analyte's overall dwell time τ is impacted by the size of the region in which mobility reduction occurs, additional simulations were performed using a set of fixed dimensional ($d_c = 400nm$, $d_e = 50nm$) and mobility reduction ($f = 0.5$, $\alpha = 0.5$) conditions, but with a varying value for σ_μ. The horizontal axis report $2\sigma_\mu/d_p$, *i.e.* the σ_μ normalized with the radius of the particle. Left panel refers to highly attractive analyte-wall interaction ($\epsilon = 6k_BT$) while right panel to repulsive ($\epsilon = 0.1k_BT$). In both cases, the plateau refer to a situation with identical potential well-depths but without mobility reduction.

Cavity diameter d_c	Repulsive ($\epsilon = 0.1k_BT$) 5 data points	Attractive ($\epsilon = 8k_BT$) 5 data points	Attractive ($\epsilon = 8k_BT$) 4 data points
400 nm	0.87	0.42	0.80
300 nm	0.82	0.11	0.45
200 nm	0.63	0.19	0.52

TABLE S1. Agreement between theoretical prediction and numerical data. To provide a more quantitative idea of how much the simulation data on the dwell time τ varies from the theoretical projections, we calculated the R^2 coefficient. Repulsive conditions ($\epsilon = 0.1k_BT$, 3D-bulk diffusion scenario) are compared with Eq.(4) of the main text while attractive case ($\epsilon = 8k_BT$, 2D-surface diffusion scenario) are compared with Eq.(6) of the main text. In the case of repulsive particle-wall interactions, there is a relatively strong agreement between the theoretical prediction and the numerical results as demonstrated by $R^2 > 0.7$ values. However, as expected from visual inspection of Fig.2b of the main text, the theoretical prediction fails in reproducing the numerical data in the entire range of cavity aperture diameters ($R^2 < 0.5$) for highly attractive interactions. Excluding the smallest aperture size (*i.e* calculating the R^2 including only 4 data points), the agreement between the theoretical prediction and the numerical data improves.

[S1] Mauro Chinappi, Misa Yamaji, Ryuji Kawano, and Fabio Cecconi. Analytical model for particle capture in nanopores elucidates competition among electrophoresis, electroosmosis, and dielectrophoresis. *ACS nano*, 14(11):15816–15828, 2020.

[S2] Alexander Y Grosberg and Yitzhak Rabin. Dna capture into a nanopore: interplay of diffusion and electrohydrodynamics. *The Journal of chemical physics*, 133(16):10B617, 2010.

[S3] Chiu Tai Andrew Wong and M Muthukumar. Polymer capture by electro-osmotic flow of oppositely charged nanopores. *The Journal of chemical physics*, 126(16):164903, 2007.

[S4] O Bénichou, D Grebenkov, P Levitz, C Loverdo, and R Voituriez. Optimal reaction time for surface-mediated diffusion. *Physical review letters*, 105(15):150606, 2010.

[S5] G Oshanin, M Tamm, and O Vasilyev. Narrow-escape times for diffusion in microdomains with a particle-surface affinity: mean-field results. *The Journal of chemical physics*, 132(23):06B607, 2010.

[S6] David Holcman and Z Schuss. Escape through a small opening: receptor trafficking in a synaptic membrane. *Journal of Statistical Physics*, 117:975–1014, 2004.

[S7] Alberto Gubbiotti, Matteo Baldelli, Giovanni Di Muccio, Paolo Malgaretti, Sophie Marbach, and Mauro Chinappi. Electroosmosis in nanopores: computational methods and technological applications. *Advances in Physics: X*, 7(1):2036638, 2022.

[S8] Igor V Grigoriev, Yurii A Makhnovskii, Alexander M Berezhkovskii, and Vladimir Yu Zitserman. Kinetics of escape through a small hole. *The Journal of chemical physics*, 116(22):9574–9577, 2002.

[S9] Terrell L Hill. Effect of rotation on the diffusion-controlled rate of ligand-protein association. *Proceedings of the National Academy of Sciences*, 72(12):4918–4922, 1975.

[S10] Crispin W Gardiner et al. *Handbook of stochastic methods*, volume 3. springer Berlin, 1985.

[S11] Sidney Redner. *A guide to first-passage processes*. Cambridge university press, 2001.